Supplementary Information

Toehold-Mediated Internal Control to Probe the Near-Field Interaction between Metallic Nanoparticle and Fluorophore

*Yan Shan Ang, and Lin-Yue Lanry Yung**

Table S1. List of DNA oligonucleotides used in this study. All sequences are shown in 5' to 3' direction.

DNA	Description	Sequence
SH	Functionalized with thiol group at 5' end for conjugation onto AuNP	/SH/ TTT TTT TTT TAG TAG GAG TTT GAG ATG AGA CGT TGA GCA GTT GAT TAG AT
10C3	MNP-fluorophore separation distance of 10 nt	CCT CAC ATC TAA TCA ACT GCT CAA CGT CTC ATC TCA AAC TCC TAC T /Cy3/
20C3	MNP-fluorophore separation distance of 20 nt	CCT CAC ATC TAA TCA ACT GCT CAA CGT CTC ATC TCA/Cy3/
29C3	MNP-fluorophore separation distance of 29 nt	CCT CAC ATC TAA TCA ACT GCT CAA CGT /Cy3/
10CS	Complementary strand to 10C3	AGT AGG AGT TTG AGA TGA GAC GTT GAG CAG TTG ATT AGA TGT GAG G
20CS	Complementary strand to 20C3	TGA GAT GAG ACG TTG AGC AGT TGA TTA GAT GTG AGG
29CS	Complementary strand to 29C3	ACG TTG AGC AGT TGA TTA GAT GTG AGG

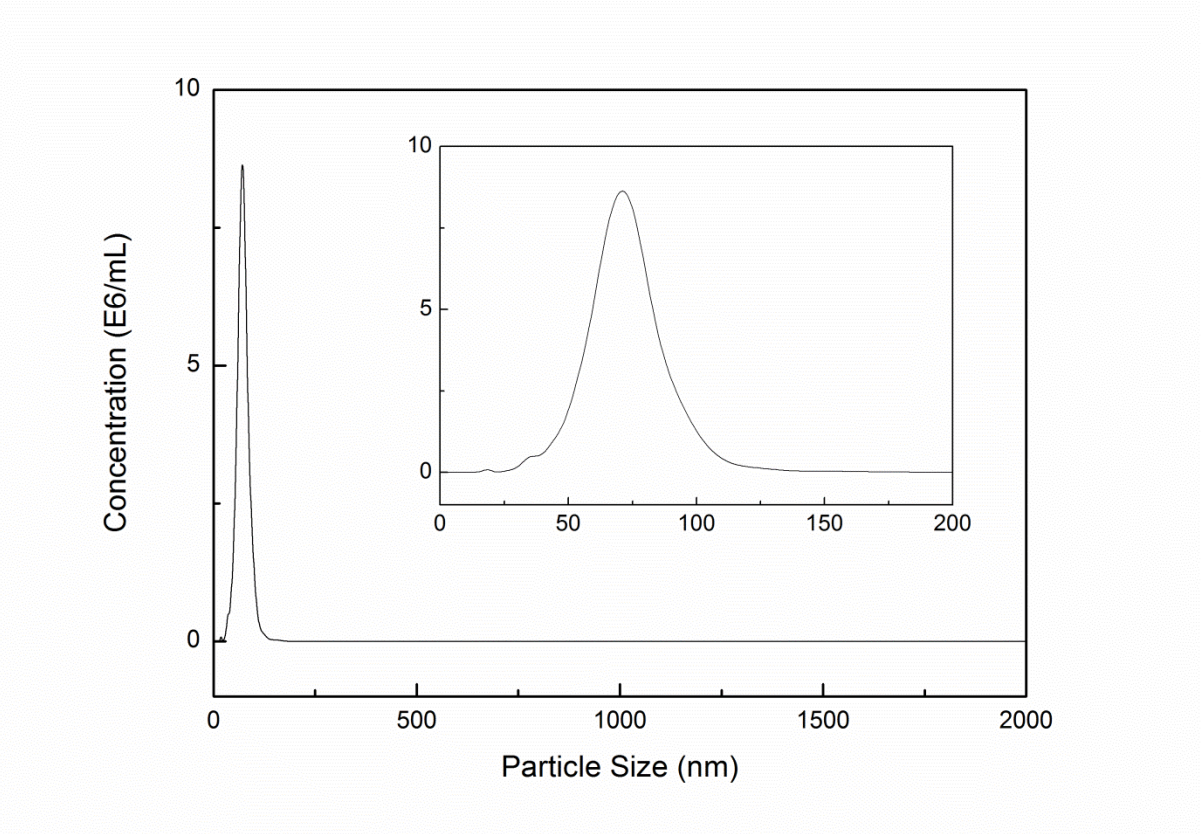

Figure S1. Size distribution of the 58 nm gold nanoparticle (AuNP) determined by nanoparticle tracking analysis (NTA, Nanosight). A narrow peak in absence of larger-size peaks was obtained, suggesting a monodispersed particle population without aggregation.

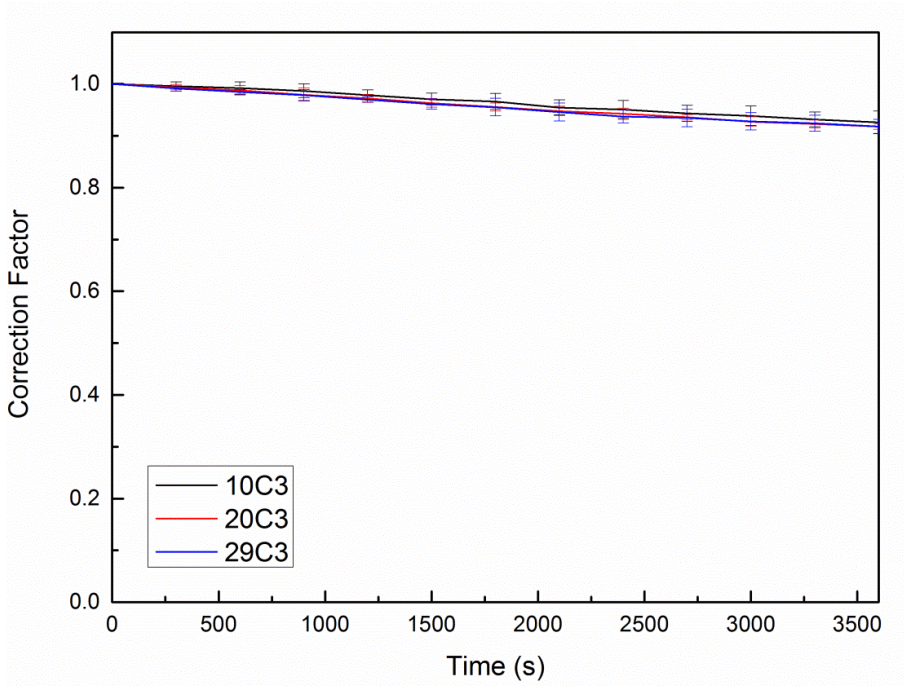

Figure S2. The extent of photobleaching was quantified over time by dividing the photoluminescence (PL) intensity at time t by that at t = 0. This ratio represents the correction factor (CF) used to estimate the actual PL intensity at each time point in absence of the photobleaching effect, i.e. measured PL intensity divided by CF. The enhancement factor (EF) was then calculated by dividing the PL intensity at t = 0 by the adjusted PL intensity at time t. At t = 0, complementary strand (CS) was added to the SH-C3 complex of three separation distances, *i.e.* 10 nt (10C3), 20 nt (20C3) and 29 nt (29C3). The PL intensity was monitored at the same measurement frequency as for the AuNP-SH-C3 complex and the effect of photobleaching was found to be invariant across sequence lengths. Strand displacement between CS and SH-C3 complex did not lead to appreciable trends of enhancement or quenching beyond that expected from photobleaching, *i.e.* gradual linear decrease with time. This served as a control set-up to prove that AuNP was the component responsible for the more drastic changes in PL intensity. All data shown are mean ± standard deviation (n = 2).

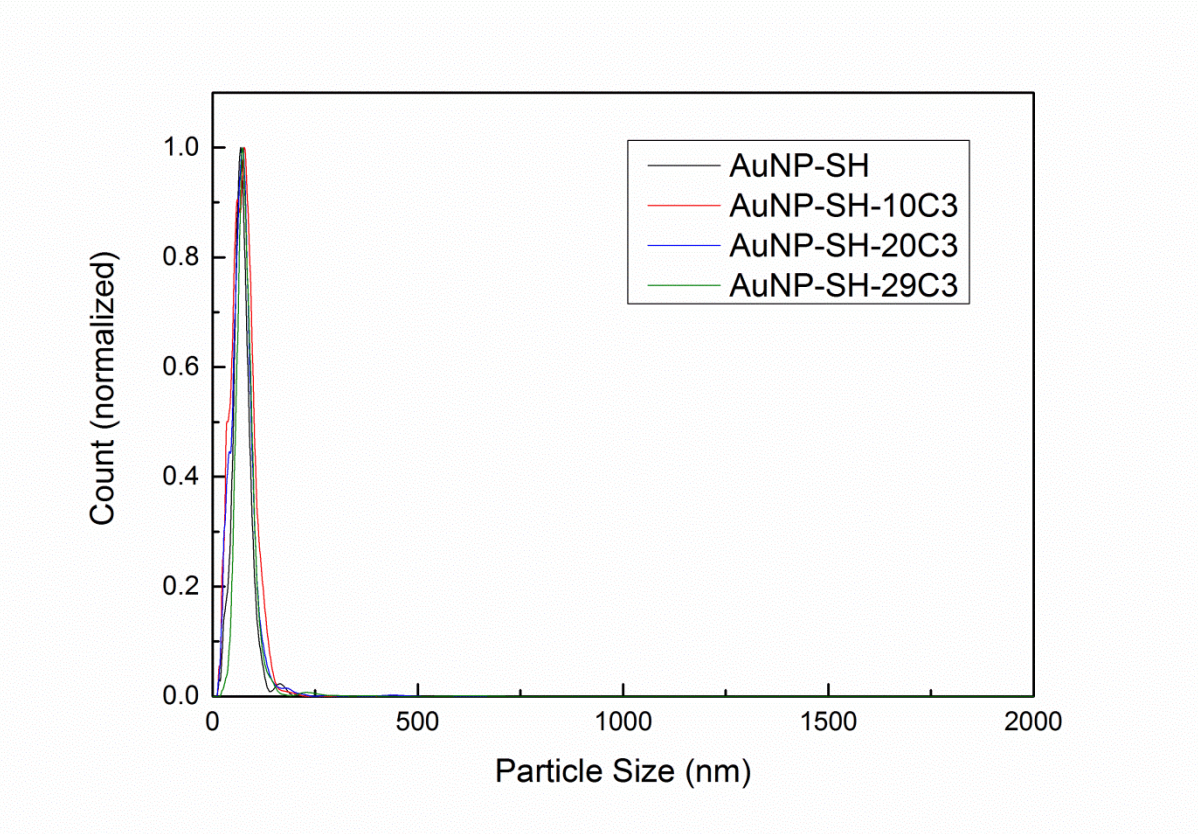

Figure S3. Size distribution of 58 nm AuNP-SH-C3 complexes of different separation distances, i.e. 10 nt (10C3), 20 nt (20C3) and 29 nt (29C3), as measured by nanoparticle tracking analysis (NTA). There was no peak in the larger size range, indicating the absence of aggregates and hence plasmonic "hot spots" in the system.

(a)

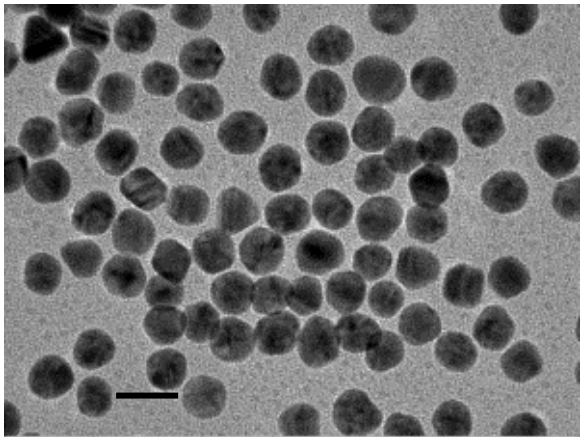

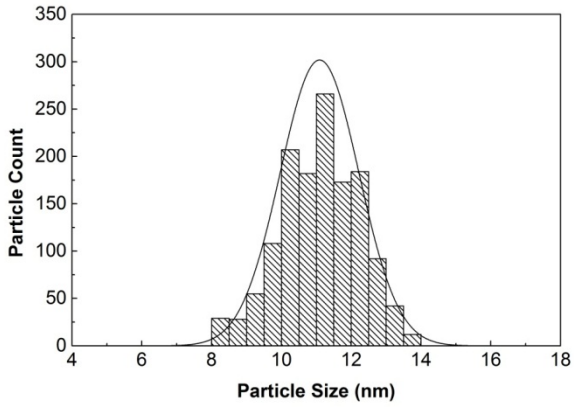

(b)

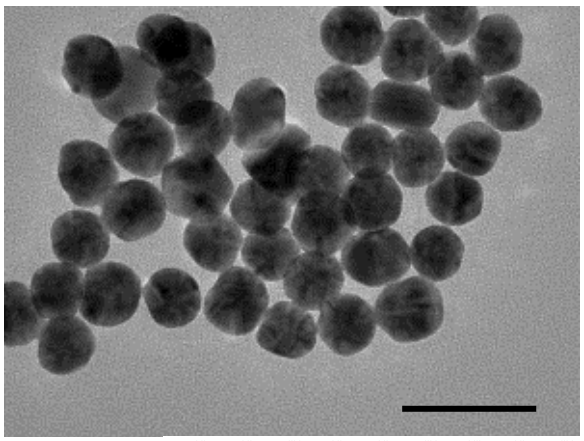

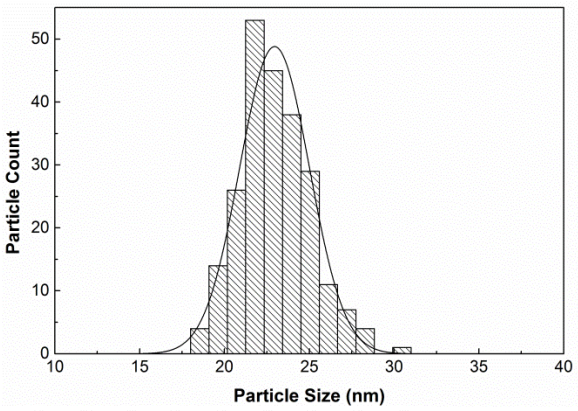

(c)

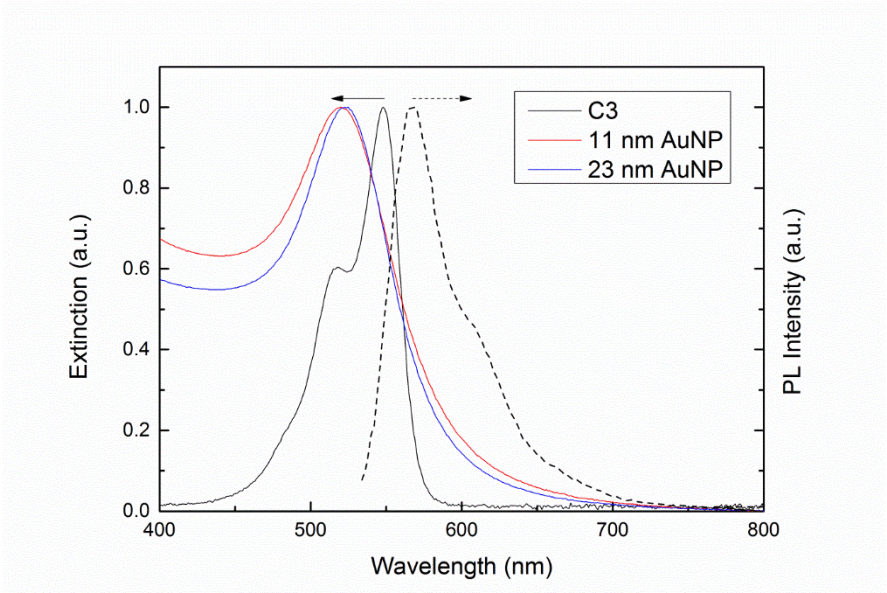

Figure S4. Transmission electron microscopy (TEM) images of (a) 11.1 ±1.1 nm (n = 1378) (scale bar = 20 nm) and (b) 23.0 ± 2.1 nm (n = 233) gold nanoparticles (AuNP) (scale bar = 50 nm) and their corresponding size distribution (right). Fairly homogeneous nanoparticle populations were obtained (PDI < 0.1). (c) Normalized extinction (solid) and emission (dotted) spectrum of Cy3-tagged DNA (C3, black), 11 nm (red) and 23 nm AuNP (blue). Large extent of spectral overlap between C3 and AuNP should facilitate the near-field interaction.